JOURNAL OF GUIDANCE, CONTROL, AND DYNAMICS
Vol. 24, No. 4, July–August 2001

Optimal Reorientation of a Multibody Spacecraft Through Joint Motion Using Averaging Theory

William Todd Cerven* and Victoria L. Coverstone†
University of Illinois at Urbana–Champaign, Urbana, Illinois 61801

The problem of reorienting a multibody spacecraft using appendage joint motion is addressed. Averaging theory shows that small periodic actuation of such appendages results in a secular change in the orientation of the multibody spacecraft. The secular variation is controllable through choice of control profiles. Using optimal control theory, an analytic control algorithm that minimizes the required control effort is developed for a four-link multibody system having zero angular momentum.

Nomenclature

$\boldsymbol{A}, \boldsymbol{B}$	=	vector coefficient functions
A_i	=	Lie algebra basis matrix
Area_{ij}	=	area defined by control curves u_i and u_j
$\boldsymbol{b}, \boldsymbol{d}$	=	joint and c.m. relative position vectors
$\boldsymbol{e}_i$	=	unit basis vector
F_{ext}	=	external forces on system
F_i, J_i	=	intermediate equation of motion functions
$\boldsymbol{g}_i$	=	ith control vector field
H	=	Hamiltonian function
$\boldsymbol{H}$	=	angular momentum
I	=	identity matrix
l_i	=	ith spacecraft link length
${}^kI_j$	=	inertia matrix of the jth component relative to the kth frame
J	=	cost
M_{ext}	=	external moments on system
m	=	number of controls of system
m_j	=	mass of jth body
m_{sys}	=	total mass of system
n	=	number of dimensions of system or number of cycles in control
$P^{\text{SO(3)}}_{[g_i, g_j]}$	=	projected Lie bracket to SO(3)
$p_i, \boldsymbol{p}$	=	periodic functions
R	=	rotation matrix
$\boldsymbol{r}$	=	link-relative position vectors
r_i	=	ith spacecraft link radius
$S(.)$	=	skew-symmetric operator
SO(3)	=	special orthogonal group of dimension 3 (rotation matrices)
T	=	period, total maneuver time
t	=	time
u_j	=	jth scalar control
$\tilde{u}_j$	=	integrated jth scalar control
X	=	generic Lie group element
$\boldsymbol{x}, \boldsymbol{y}$	=	state variables
$Z(t)$	=	matrix exponential function
ε	=	multiplier $\ll 1$
$\boldsymbol{\theta}^*$	=	nominal shape
$\boldsymbol{\mu}_y$	=	y Lagrange multiplier
$\boldsymbol{\mu}_\theta$	=	θ Lagrange multiplier
ξ, η, ζ	=	body-fixed axes
$\boldsymbol{\rho}$	=	c.m. position vectors
ϕ^t_x	=	flow of X at time t
ψ, ϕ, θ	=	3–2–1 Euler angles
${}^k\boldsymbol{\Omega}_{ij}$	=	angular velocity of the ith body relative to the jth, referenced to the kth coordinate frame
$[\boldsymbol{Area}_{ij}]$	=	vector of areas defined by curves u_i and u_j, for all i, j
$[.,.]$	=	Lie bracket
$\lvert\cdot\rvert$	=	vector Frobenius norm
$\lVert\cdot\rVert$	=	norm

Introduction

WITH NASA's interest in faster, smaller, and cheaper missions, engineers have increasingly been forced to look for new ways to meet mission objectives with fewer resources. Commonly, the most limiting factor for a spacecraft is mass. Thus, engineers are continually searching for ways to reduce mass, particularly in the areas of propellant and excess redundancy. Although this is a dilemma, advances in spacecraft technology have introduced some intriguing capabilities that have yet to be exploited.

The configurations of modern spacecraft are far removed from Sputnik's design. Many modern spacecraft are equipped with actuated solar arrays, antennas, and instrument platforms. Even robotic arms are becoming more common inasmuch as the new International Space Station will be heavily dependent on them. These actuated appendages are a bane for most control engineers because they introduce perturbations to the system that must be handled by the attitude control system, often costing precious propellant in the process. Ironically, this same property, the ability of an actuated appendage to perturb the system, is what also provides control opportunities. Through judicious control of the actuations, the resulting orientation of the spacecraft can be controlled. This provides a valuable alternative to thrusters by allowing reorientation without propellant usage. It also provides a backup for failure in primary systems such as thrusters and wheels.

The problem of reorienting a multibody spacecraft is analogous to that of reorienting a falling cat. Somehow, a cat, when dropped, (almost) always lands on its feet. From classical mechanics, we know angular momentum is conserved; therefore, when a cat reorients itself from being dropped from a rest position upside-down, one might wonder how this is dynamically possible. The motion of the cat as it falls is the answer. From a control point of view, this sort of system falls into the class of underactuated systems, those which have fewer controls than degrees of freedom. As angular momentum is conserved, this system is also kinematic and driftless, for example, the states are changing only when the controls, joint movements in this case, are active. Dynamically, this falling cat problem is the same as that for any rigid multibody system with no external torques acting on the system. Kane and Scher[1] addressed this through dynamic systems theory and then applied it to the problem of astronaut reorientation.[2] Krishnaprasad[3] provided a general framework for addressing reconfiguration of multibody systems. Near-optimal and optimal controls were applied to the cat and spacecraft problems by Fernandes et al.[4] and Coverstone-Carroll and Wilkey.[5] One of the problems with these solutions to the rigid-multibody system reconfiguration problem is that the controls

Received 31 March 2000; revision received 4 October 2000; accepted for publication 17 November 2000.

*Graduate Student, Department of Aeronautical and Astronautical Engineering, 306 Talbot Laboratory; w-cerven@uiuc.edu. Student Member AIAA.

†Associate Professor, Department of Aeronautical and Astronautical Engineering, 306 Talbot Laboratory; vcc@uiuc.edu. Senior Member AIAA.

are numerical in nature. Therefore, the controls are not easily recomputed for differing mechanical systems or desired final conditions. Rui[6] changed this by introducing a method to develop analytic controls of multibody systems using averaging and nonlinear systems theory. This methodology follows control theory developed by Leonard and Krishnaprasad[7,8] and Leonard,[9] who, in turn, were inspired by some of Brockett's[10] work. They[7–9] show that periodic small controls can be used to provide a secular state variation in any direction. Through use of this theory, it is possible to control an averaged system exactly and an actual system approximately.

This paper bypasses traditional numerical optimization such as that in Coverstone-Carroll and Wilkey[5] as well as the Ritz approximation-based method of Fernandes et al.[4] by taking advantage of the structure used by Rui[6] and Rui et al.[11] When small periodic joint velocity controls are assumed so that higher-order effects could be neglected (a reasonable assumption, given geometric and mechanical constraints on spacecraft appendages), Rui developed various control schemes to reorient spacecraft. By the use of the same assumptions, this paper applies optimal control theory to obtain analytically a control algorithm that minimizes actuator energy expenditure, thus providing a marked improvement in efficiency over previously developed controls. Because of the analytic nature of these controls, given an accurate spacecraft model, control histories can be quickly and easily computed to effect an arbitrary reorientation.

Background

Brockett[10] applied averaging theory to nonlinear systems to show that the states of a driftless system under small periodic controls of period T and suitable initial conditions show small periodic motion plus higher-order secular motion. Specifically, given a system

$$\dot{\boldsymbol{x}} = \boldsymbol{g}_1(\boldsymbol{x})u_1 + \boldsymbol{g}_2(\boldsymbol{x})u_2$$

where

$$\boldsymbol{u} = \mathcal{O}(\varepsilon), \qquad \tilde{u}_i(T) = 0 \tag{1}$$

given

$$\varepsilon \ll 1, \qquad \tilde{u}_i = \int_{\tau=0}^{t} u_i(\tau)\,\mathrm{d}\tau$$

the state history $x(t)$ can be written as

$$\boldsymbol{x}(t) = \boldsymbol{x}_0 + \boldsymbol{p}(t) + [\boldsymbol{g}_1, \boldsymbol{g}_2]\frac{\text{Area}_{12}}{T}t + \mathcal{O}(\varepsilon^3)$$

$$[\boldsymbol{g}_1, \boldsymbol{g}_2] = \frac{\partial \boldsymbol{g}_2}{\partial \boldsymbol{x}}\boldsymbol{g}_1 - \frac{\partial \boldsymbol{g}_1}{\partial \boldsymbol{x}}\boldsymbol{g}_2 \tag{2}$$

given

$$\text{Area}_{ij} = \int_{\tau=0}^{T} \tilde{u}_i \dot{\tilde{u}}_j\,\mathrm{d}\tau = \frac{1}{2}\int_{\tau=0}^{T} \tilde{u}_i \dot{\tilde{u}}_j - \tilde{u}_j \dot{\tilde{u}}_i\,\mathrm{d}\tau$$

where x_0 is the initial state, $\boldsymbol{p}(t)$ is a periodic vector function, $[\boldsymbol{g}_1, \boldsymbol{g}_2]$ is the first-order Lie bracket of the control vectors $\boldsymbol{g}_1$ and $\boldsymbol{g}_2$, and Area_{12} is the area defined by the curves $\tilde{u}_1$ and $\tilde{u}_2$ by Green's theorem. Therefore, careful choice of periodic controls allows controllability along the direction of the Lie bracket. Expansion to higher-order terms allows controllability along higher-order Lie brackets as well. Any n-dimensional system of the form (3) is controllable providing it satisfies the Lie algebra controllability rank condition (4):

$$\dot{\boldsymbol{x}} = \sum_{i=1}^{m} \boldsymbol{g}_i(x)u_i \tag{3}$$

$$\text{rank}\{\boldsymbol{g}_i, [\boldsymbol{g}_i, \boldsymbol{g}_j], [\boldsymbol{g}_k, [\boldsymbol{g}_i, \boldsymbol{g}_j]], [\boldsymbol{g}_l, [\boldsymbol{g}_k, [\boldsymbol{g}_i, \boldsymbol{g}_j]]], \ldots, \forall i, j, k, l, \ldots\} = n \tag{4}$$

Leonard and Krishnaprasad[7,8] and Leonard[9] took Brockett's[10] work a step further and applied averaging theory to Lie groups to approximate and control underactuated Lie group systems, including SO(3), of the form

$$\dot{X} = XU, \qquad U = \sum_{i=1}^{m} A_i(x)u_i \tag{5}$$

where X is a generic Lie group element of dimension n and A_i, $i = 1, \ldots, n$ is a basis of $\ell n(X)$, where $\ell n(\,)$ is the inverse of the exponential mapping for Lie groups. Because the controls fit the constraints in Eq. (1), Leonard showed that these systems provide a periodic secular response due to small periodic controls. The state history then is described by

$$Z(t) = S(\tilde{\boldsymbol{u}}(t)) + \frac{t}{T}\sum_{i,j=1}^{m} \text{Area}_{ij}(T)[A_i, A_j] + \mathcal{O}(\varepsilon^3)$$

$$X(t) = e^{z(t)}, \qquad S(\boldsymbol{V}) = \begin{bmatrix} 0 & -V_3 & V_2 \\ V_3 & 0 & -V_1 \\ -V_2 & V_1 & 0 \end{bmatrix} \tag{6}$$

In Refs. 7 and 9, there is a detailed proof of these properties. For these matrix Lie group systems, the Lie bracket, when simplified, is shown to be the matrix commutator:

$$[A_1, A_2] = A_1A_2 - A_2A_1 \tag{7}$$

Multibody Spacecraft Mathematical Model

Whereas Leonard's[9] theory was developed for matrix Lie group systems, Rui[6] has applied these concepts to multibody spacecraft, for which a mathematical model is now derived. Consider the system in Fig. 1. The inertial coordinate frame is represented by the axes $X_IY_IZ_I$, whereas the coordinate frame of the system center of mass is $X_{\text{cm}}Y_{\text{cm}}Z_{\text{cm}}$ and has the system center of mass as its origin. This coordinate frame has axes parallel to that of the inertial frame, and its origin is defined by ρ_{cm}. The axes $\xi_i\eta_i\zeta_i$ represent the body-fixed axes of component L_i, with its origin at the center of mass of that body. Here, the base body is denoted subscript 0, whereas links are numbered from 1 to m. The vectors $\boldsymbol{\rho}_i$ and $\boldsymbol{r}_i$ denote the

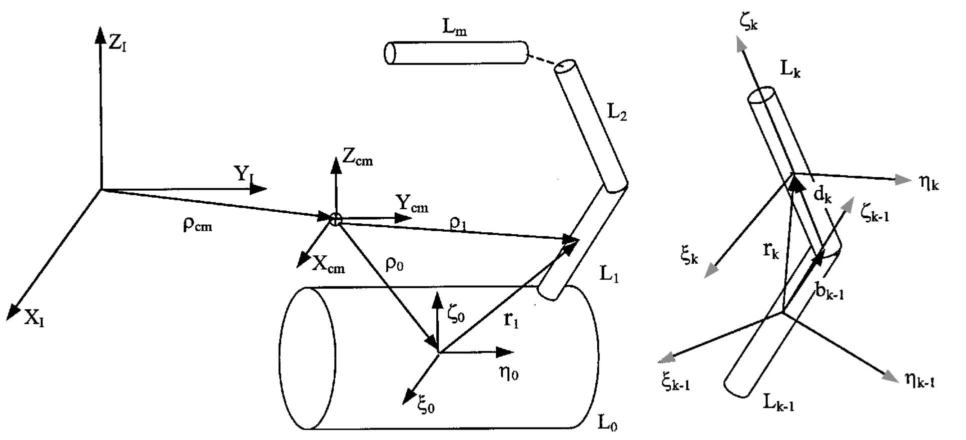

Fig. 1 Multibody spacecraft system.

position vectors of a link's center of mass to the system center of mass reference frame and the previous link's frame, respectively.

The $\boldsymbol{b}$ vector represents the next joint position relative to the body center of mass, whereas the $\boldsymbol{d}$ vector defines the body center of mass position relative to the last joint. Thus, the following condition is satisfied:

$$\boldsymbol{r}_k = \boldsymbol{b}_{k-1} + \boldsymbol{d}_k \tag{8}$$

Let $R_{i,j} \in \mathrm{SO}(3)$ be the rotation matrix from the jth coordinate frame to the ith coordinate frame. For example, for a vector $\boldsymbol{V}_j$ in the jth coordinate frame,

$$\boldsymbol{V}_i = R_{i,j}\boldsymbol{V}_j \tag{9}$$

Let the angular velocity vector between the inertial and base body frame, expressed in the base body frame, be denoted by ${}^0\Omega_{I,0}$. This is related to the rotation matrix $R_{I,0}$ by

$$\dot{R}_{I,0} = R_{I,0}S\left({}^0\Omega_{I,0}\right) \tag{10}$$

In this paper, the rotation matrix $R_{I,0}$ will often be denoted as R, for sake of simplicity. More generally, let the angular velocity vector between the ith and jth coordinate frame, expressed in the jth coordinate frame, be denoted by ${}^j\boldsymbol{\Omega}_{i,j}$ (note that left superscripts refer to the reference frame). This is related to the rotation matrix $R_{i,j}$ by

$$\dot{R}_{i,j} = R_{i,j}S\left({}^j\boldsymbol{\Omega}_{i,j}\right) \tag{11}$$

The angular velocity of the kth link relative to the inertial frame can be expressed as

$${}^k\boldsymbol{\Omega}_{I,k} = (R_{0,k})^T\left({}^0\boldsymbol{\Omega}_{I,0} + \sum_{i=1}^{k}{}^0\boldsymbol{\Omega}_{i-1,i}\right) \tag{12}$$

where $R_{0,k}$ is defined as

$$R_{0,k} = R_{0,1}R_{1,2}, \ldots, R_{k-1,k} \tag{13}$$

A joint constrains the relative motion of the two links it connects. In other words, it constrains $R_{k-1,k}$. For 3–2–1 (ψ, ϕ, θ) Euler angles,

$$R_{k-1,k} = \begin{bmatrix} \cos\psi_k\cos\phi_k & -\sin\psi_k\cos\theta_k + \cos\psi_k\sin\phi_k\sin\theta_k & \sin\psi_k\sin\theta_k + \cos\psi_k\sin\phi_k\cos\theta_k \\ \sin\psi_k\cos\phi_k & \cos\psi_k\cos\theta_k + \sin\psi_k\sin\phi_k\sin\theta_k & -\cos\psi_k\sin\theta_k + \sin\psi_k\sin\phi_k\cos\theta_k \\ -\sin\phi_k & \cos\phi_k\sin\theta_k & \cos\phi_k\cos\theta_k \end{bmatrix} \tag{14}$$

For a revolute joint, ψ and ϕ are defined to be fixed, whereas θ is the joint angle. This constraint can be expressed in terms of the angular velocity, where

$${}^k\dot{\boldsymbol{\Omega}}_{k-1,k} = \boldsymbol{e}_1\dot{\theta}_k \tag{15}$$

$$\boldsymbol{e}_1 = [1 \quad 0 \quad 0]^T \tag{16}$$

The angular momentum of the system about its center of mass can be expressed in the base body reference frame $\xi_0\eta_0\zeta_0$ as

$${}^0\boldsymbol{H} = {}^0I_0\left({}^0\boldsymbol{\Omega}_{I,0}\right) + m_0S\left({}^0\boldsymbol{\rho}_0\right){}^0\dot{\boldsymbol{\rho}}_0 + \sum_{j=1}^{m}{}^0I_j\left({}^0\boldsymbol{\Omega}_{I,j}\right) + \sum_{j=1}^{m}m_jS\left({}^0\boldsymbol{\rho}_j\right){}^0\dot{\boldsymbol{\rho}}_j \tag{17}$$

where m_0 and m_j are the masses of the base body and link L_j whereas ${}^0I_0$ and ${}^0I_j$ are the inertia matrices of the base body and link L_j expressed in the base body frame. The inertia matrix for link L_j in the base body frame can be related to the L_j body-fixed frame through rotation matrices as

$${}^0I_j = R_{0,j}\left({}^jI_j\right)(R_{0,j})^T \tag{18}$$

To solve Eq. (17), expressions for $\boldsymbol{\rho}_j$ and $\boldsymbol{\rho}_0$ along with their derivatives with respect to time must be developed. This derivation is not included here for brevity, but may be found in detail in Ref. 12. The expressions are

$${}^I\boldsymbol{\rho}_0 = -\frac{1}{m_{\mathrm{sys}}}\sum_{i=1}^{m}\left(\left(\sum_{j=i}^{m}m_j\right)\left(R_{I,i-1}\left({}^{i-1}\boldsymbol{b}_{i-1}\right) + R_{I,i}\left({}^i\boldsymbol{d}_i\right)\right)\right)$$

$${}^0\boldsymbol{\rho}_0 = -\frac{1}{m_{\mathrm{sys}}}\sum_{i=1}^{m}\left(\left(\sum_{j=i}^{m}m_j\right)\left(R_{0,i-1}\left({}^{i-1}\boldsymbol{b}_{i-1}\right) + R_{0,i}\left({}^i\boldsymbol{d}_i\right)\right)\right) \tag{19}$$

$$\begin{aligned}{}^0\dot{\boldsymbol{\rho}}_0 = {}& \frac{1}{m_{\mathrm{sys}}}\sum_{i=1}^{m}\left(\left(\sum_{j=i}^{m}m_j\right)\left[R_{0,i-1}S\left({}^{i-1}\boldsymbol{b}_{i-1}\right)(R_{0,i-1})^T + R_{0,i}S\left({}^i\boldsymbol{d}_i\right)(R_{0,i})^T\right]\right)\left({}^0\boldsymbol{\Omega}_{I,0}\right) \\ & + \frac{1}{m_{\mathrm{sys}}}\sum_{k=1}^{m-1}\left[\sum_{i=k}^{m-1}\sum_{j=i+1}^{m}m_jR_{0,i}S\left({}^i\boldsymbol{b}_i\right)(R_{0,i})^T + \sum_{i=k}^{m}\sum_{j=i}^{m}m_jR_{0,i}S\left({}^i\boldsymbol{d}_i\right)(R_{0,i})^T\right]\left({}^0\boldsymbol{\Omega}_{k-1,k}\right) \\ & + \frac{1}{m_{\mathrm{sys}}}R_{0,m}S\left({}^m\boldsymbol{d}_m\right)(R_{0,m})^T\left({}^0\boldsymbol{\Omega}_{m-1,m}\right)\end{aligned} \tag{20}$$

$$\begin{aligned}{}^0\dot{\boldsymbol{\rho}}_k = {}& {}^0\dot{\boldsymbol{\rho}}_0 - \sum_{i=1}^{m}\left[R_{0,i-1}S\left({}^{i-1}\boldsymbol{b}_{i-1}\right)(R_{0,i-1})^T + R_{0,i}S\left({}^i\boldsymbol{d}_i\right)(R_{0,i})^T\right]\left({}^0\boldsymbol{\Omega}_{I,0}\right) \\ & - \sum_{s=1}^{m-1}\left[\sum_{i=s}^{m-1}R_{0,i-1}S\left({}^{i-1}\boldsymbol{b}_{i-1}\right)(R_{0,i-1})^T + \sum_{i=s}^{m}R_{0,i}S\left({}^i\boldsymbol{d}_i\right)(R_{0,i})^T\right]\left({}^0\boldsymbol{\Omega}_{s-1,s}\right) \\ & - R_{0,k}S\left({}^k\boldsymbol{d}_k\right)(R_{0,k})^T\left({}^0\boldsymbol{\Omega}_{k-1,k}\right)\end{aligned} \tag{21}$$

When Eqs. (18–21) are substituted into Eq. (17), a final expression for the angular momentum can be written as

$${}^0H_{\mathrm{cm}} = J_0\left({}^0\boldsymbol{\Omega}_{I,0}\right) + \sum_{j=1}^{m}J_j\left({}^j\boldsymbol{\Omega}_{j-1,j}\right) \tag{22}$$

The matrices J_0 and J_j are defined as

$$\begin{aligned}J_0 = {}& {}^0I_0 + \sum_{k=1}^{m}R_{0,k}\left({}^kI_k\right)(R_{0,k})^T \\ & + \frac{1}{m_{\mathrm{sys}}}\left(m_0S\left({}^0\boldsymbol{\rho}_0\right) + \sum_{j=1}^{m}m_jS\left({}^0\boldsymbol{\rho}_j\right)\right)\sum_{i=1}^{m}\left(\left(\sum_{j=i}^{m}m_j\right) \times\left[R_{0,i-1}S\left({}^{i-1}\boldsymbol{b}_{i-1}\right)(R_{0,i-1})^T + R_{0,i}S\left({}^i\boldsymbol{d}_i\right)(R_{0,i})^T\right]\right) \\ & + \sum_{i=1}^{m}\left(\left(\sum_{j=i}^{m}m_jS\left({}^0\boldsymbol{\rho}_j\right)\right)\left[R_{0,i-1}S\left({}^{i-1}\boldsymbol{b}_{i-1}\right)(R_{0,i-1})^T + R_{0,i}S\left({}^i\boldsymbol{d}_i\right)(R_{0,i})^T\right]\right)\end{aligned} \tag{23}$$

$$J_j = \left\{ \sum_{k=1}^{m} R_{0,k}\left({}^k I_k\right)(R_{0,k})^T + \frac{1}{m_{\text{sys}}}\left(m_0 S\left({}^0\boldsymbol{\rho}_0\right) \sum_{j=1}^{m} m_j S\left({}^0\boldsymbol{\rho}_j\right)\right) \right.$$
$$\times \left[\sum_{i=1}^{m-1} \left(\left(\sum_{j=i+1}^{m} m_j \right) R_{0,i} S\left({}^i\boldsymbol{b}_i\right)(R_{0,i})^T \right) + \sum_{i=1}^{m} \left(\left(\sum_{j=i}^{m} m_j \right) R_{0,i} S\left({}^i\boldsymbol{d}_i\right)(R_{0,i})^T \right) \right]$$
$$- \sum_{i=1}^{m-1} \left(\left(\sum_{j=i+1}^{m} m_j S\left({}^0\boldsymbol{\rho}_j\right) \right) R_{0,i} S\left({}^i\boldsymbol{b}_i\right)(R_{0,i})^T \right)$$
$$\left. - \sum_{i=1}^{m} \left(\left(\sum_{j=i}^{m} m_j S\left({}^0\boldsymbol{\rho}_j\right) \right) R_{0,i} S\left({}^i\boldsymbol{d}_i\right)(R_{0,i})^T \right) \right\} R_{0,j} \qquad j = 1, \ldots, m-1 \tag{24}$$

$$J_m = \left\{ R_{0,k}\left({}^k I_k\right)(R_{0,k})^T + \frac{1}{m_{\text{sys}}}\left(m_0 S\left({}^0\boldsymbol{\rho}_0\right) + \sum_{j=1}^{m} m_j S\left({}^0\boldsymbol{\rho}_j\right)\right) m_m R_{0,m} S\left({}^m\boldsymbol{d}_m\right)(R_{0,m})^T \right.$$
$$\left. - m_m S\left({}^0\rho_n\right) R_{0,m} S\left({}^m\boldsymbol{d}_m\right)(R_{0,m})^T \right\} R_{0,m} \tag{25}$$

Equations of Motion

The equations of motion for this multibody spacecraft are derived from Newton's second law. For the total force F_{ext} and torque M_{ext} acting on the system, this can be written as

$${}^I\dot{\boldsymbol{p}} = {}^I\boldsymbol{F}_{\text{ext}}, \qquad {}^I\dot{\boldsymbol{H}}_{\text{cm}} = {}^I\boldsymbol{M}_{\text{ext}} \tag{26}$$

The total system linear momentum is represented as $\boldsymbol{p}$ and is defined by

$${}^I\boldsymbol{p} = m_{\text{sys}}\left({}^I\dot{\boldsymbol{\rho}}_{\text{cm}}\right) \tag{27}$$

$\boldsymbol{H}_{\text{cm}}$ is the total system angular momentum about its center of mass as defined in Eq. (22). Assuming that $\boldsymbol{F}_{\text{ext}}$ and $\boldsymbol{M}_{\text{ext}}$ are unrelated to the spacecraft states, the rotational and translational equations of motion are uncoupled. However, whereas this makes the translational equations of motion easy to solve using Eqs. (26) and (27), the rotational equations of motion are still not so simple. When Newton's second law for angular momentum in the body frame is rewritten,

$$R_{I,0}{}^0\boldsymbol{M}_{\text{ext}} = \dot{R}_{I,0}\left({}^0\boldsymbol{H}_{\text{cm}}\right) + R_{I,0}\left({}^0\dot{\boldsymbol{H}}_{\text{cm}}\right) \tag{28}$$

the time rate of change of ${}^0H_{\text{cm}}$ is solved for, and Eq. (10) is used,

$${}^0\dot{\boldsymbol{H}}_{\text{cm}} = {}^0\boldsymbol{H}_{\text{cm}} \times \left({}^0\boldsymbol{\Omega}_{I,0}\right) + {}^0\boldsymbol{M}_{\text{ext}} \tag{29}$$

The angular velocity of the base body frame can then be found from Eq. (22):

$${}^0\boldsymbol{\Omega}_{I,0} = (J_0)^{-1}\left({}^0\boldsymbol{H}_{\text{cm}}\right) + \sum_{j=1}^{m} \boldsymbol{F}_j\dot{\theta}_j, \qquad \boldsymbol{F}_j = -(J_0)^{-1}J_j\boldsymbol{e}_1 \tag{30}$$

In this system, u_j (for all $j = 1, \ldots, m$) are the joint velocity controls. For a system with zero external moments and zero initial angular momentum, the angular momentum is zero for all time. When all joints are actuated, the rotational equations of motion then simplify to

$${}^0\boldsymbol{H}_{\text{cm}} = \text{const} = \boldsymbol{0} \tag{31}$$

$$\dot{R}_{I,0} = R_{I,0}\sum_{j=1}^{m} S(\boldsymbol{F}_j(\boldsymbol{\theta}))u_j \tag{32}$$

$$\dot{\theta}_j = u_j \tag{33}$$

An advantage to this formulation of the equations of motion is that, while taking the form of a kinematic model (no drift term), they incorporate the full dynamics of the system when no external torques are present. Thus, conservation of angular momentum allows the reduced dynamics evidenced in Eqs. (32) and (33). Such a system simplifies the control problem remarkably. Although the function $\boldsymbol{F}_j(\boldsymbol{\theta})$ in Eq. (32) is very complicated, commercial mathematics software makes computation of these equations much easier. This formulation thus provides a ready basis for the development of joint actuation controls to reorient the spacecraft.

Multibody Spacecraft Lie Bracket Control

When this formulation of the rotational equations of motion is used, Leonard's[9] concepts can be applied to a multibody spacecraft. Once again, the controls are assumed to fit the constraints of Eq. (1). The vector fields of system (32) are defined as

$$\boldsymbol{g}_i(R, \theta) = \begin{bmatrix} RS(\boldsymbol{F}_i(\boldsymbol{\theta})) \\ \boldsymbol{e}_i \end{bmatrix}, \qquad \forall i = 1, \ldots, m \qquad (\text{note: } R = R_{I,0}) \tag{34}$$

where $\boldsymbol{e}_i$ is the ith unit basis vector in R^n, and where the vector field $\boldsymbol{g}_i$ exists in the tangent space of $\text{SO}(3) \times T^m$. Define the flow, ϕ^t, of the vector fields to be the solution to the differential equation (35). The Lie bracket can then be defined in terms of the flow and found as follows:

$$\dot{\boldsymbol{x}} = \boldsymbol{g}_i(\boldsymbol{x}), \qquad \phi^t_{gi} = \boldsymbol{x} \tag{35}$$

$$[\boldsymbol{g}_i, \boldsymbol{g}_j] = \left.\frac{\mathrm{d}}{\mathrm{d}t}\right|_{t=0} \left\{ \left.\frac{\mathrm{d}}{\mathrm{d}\tau}\right|_{\tau=0} \phi^t_{gi}\left(\phi^\tau_{gj}(R, \boldsymbol{\theta})\right) - \left.\frac{\mathrm{d}}{\mathrm{d}\tau}\right|_{\tau=0} \phi^t_{gj}\left(\phi^\tau_{gi}(R, \boldsymbol{\theta})\right) \right\}$$
$$= \left.\frac{\mathrm{d}}{\mathrm{d}t}\right|_{t=0} \left\{ \left[\left.\frac{\mathrm{d}}{\mathrm{d}\tau}\right|_{\tau=0} \begin{matrix} R\exp^{S(\boldsymbol{F}_j(\boldsymbol{\theta}))\tau + S[\mathcal{O}(\tau^2)]}\, e^{S(\boldsymbol{F}_i(\boldsymbol{\theta}+\boldsymbol{e}_j\tau))t + S[\mathcal{O}(t^2)]} \\ \theta + \boldsymbol{e}_j\tau + \boldsymbol{e}_i t \end{matrix} \right] - \left[\left.\frac{\mathrm{d}}{\mathrm{d}\tau}\right|_{\tau=0} \begin{matrix} R\exp^{S(\boldsymbol{F}_i(\boldsymbol{\theta}))\tau + S[\mathcal{O}(\tau^2)]}\, e^{S(\boldsymbol{F}_j(\boldsymbol{\theta}+\boldsymbol{e}_i\tau))t + S[\mathcal{O}(t^2)]} \\ \boldsymbol{\theta} + \boldsymbol{e}_i\tau + \boldsymbol{e}_j t \end{matrix} \right] \right\}$$
$$= \left.\frac{\mathrm{d}}{\mathrm{d}t}\right|_{t=0} \left\{ \begin{bmatrix} RS(\boldsymbol{F}_j(\boldsymbol{\theta}))e^{S(\boldsymbol{F}_i(\boldsymbol{\theta}))t + S[\mathcal{O}(t^2)]} + R\exp^{S(\boldsymbol{F}_i(\boldsymbol{\theta}))t + S[\mathcal{O}(t^2)]} S\left(\frac{\partial \boldsymbol{F}_i}{\partial \boldsymbol{\theta}}(\boldsymbol{\theta})\boldsymbol{e}_j\right)t \\ \boldsymbol{e}_j \end{bmatrix} \right.$$
$$\left. - \begin{bmatrix} RS(\boldsymbol{F}_i(\boldsymbol{\theta}))e^{S(\boldsymbol{F}_j(\boldsymbol{\theta}))t + S[\mathcal{O}(t^2)]} + R\exp^{S(\boldsymbol{F}_j(\boldsymbol{\theta}))t + S[\mathcal{O}(t^2)]} S\left(\frac{\partial \boldsymbol{F}_j}{\partial \boldsymbol{\theta}}(\boldsymbol{\theta})\boldsymbol{e}_i\right)t \\ \boldsymbol{e}_i \end{bmatrix} \right\} \tag{36}$$

$$[\boldsymbol{g}_i, \boldsymbol{g}_j] = \begin{bmatrix} RS\left(\boldsymbol{F}_j(\boldsymbol{\theta}) \times \boldsymbol{F}_i(\boldsymbol{\theta}) + \dfrac{\partial \boldsymbol{F}_i}{\partial \boldsymbol{\theta}_j}(\boldsymbol{\theta}) - \dfrac{\partial \boldsymbol{F}_j}{\partial \boldsymbol{\theta}_i}(\boldsymbol{\theta})\right) \\ \boldsymbol{0} \end{bmatrix} \tag{37}$$

The projections of these Lie brackets on the tangent space of SO(3) (the portion of the Lie brackets corresponding to the rotation matrix differential equation) are the quantities that will be used to determine the averaged SO(3) system solution. The joints are fully actuated with projected Lie brackets of zero and can be easily modeled. Define the projections as

$$P^{\mathrm{SO(3)}}_{[g_i, g_j]} = S\left(\boldsymbol{F}_j(\boldsymbol{\theta}) \times \boldsymbol{F}_i(\boldsymbol{\theta}) + \frac{\partial \boldsymbol{F}_i}{\partial \boldsymbol{\theta}_j}(\boldsymbol{\theta}) - \frac{\partial \boldsymbol{F}_j}{\partial \boldsymbol{\theta}_i}(\boldsymbol{\theta})\right) \tag{38}$$

By exponential expansion, the final orientation can be expressed in terms similar to Eq. (6):

$$Z(T) = P^{\mathrm{SO(3)}}_{[g_1, g_2]}\mathrm{Area}_{12} + P^{\mathrm{SO(3)}}_{[g_3, g_1]}\mathrm{Area}_{31} + P^{\mathrm{SO(3)}}_{[g_2, g_3]}\mathrm{Area}_{23} + S\left(\mathcal{O}\left(\int_0^T \|\boldsymbol{\theta}\|^2 u_i \,\mathrm{d}t\right)\right) + Z_0 \tag{39}$$

$$Z(T) = P^{\mathrm{SO(3)}}_{[g_1, g_2]}\mathrm{Area}_{12} + P^{\mathrm{SO(3)}}_{[g_3, g_1]}\mathrm{Area}_{31} + P^{\mathrm{SO(3)}}_{[g_2, g_3]}\mathrm{Area}_{23} + Z_0 + \mathcal{O}(\varepsilon^3)$$

$$R(T) = e^{Z(T)} \tag{40}$$

Optimal Control Derivation

One of the major dilemmas in using averaging methods and Lie brackets to control nonlinear systems is that the path of control development is quite varied, as can be seen in differing approaches by Leonard and Krisnaprasad,[7,8] Leonard[9] and Rui.[6] In this paper, optimal control theory is used to achieve a control that will result in a desired reorientation in a far more efficient manner than those that have been previously proposed.

System and Constraint Setup

The equations of motion of the multibody system are given by Eqs. (32) and (33). Provided that the Lie algebra rank controllability condition is satisfied by the first-order projected Lie brackets, a desired reorientation from the orientation $R(0) \in \mathrm{SO(3)}$ to a final orientation $R(T)$ can be achieved. Note that the parameter T is used for the final time. The system final orientation is given by Eq. (31), which can be rewritten as

$$Z(T) = P^{\mathrm{SO(3)}}_{[g_1, g_2]}\mathrm{Area}_{12} + P^{\mathrm{SO(3)}}_{[g_3, g_1]}\mathrm{Area}_{31} + P^{\mathrm{SO(3)}}_{[g_2, g_3]}\mathrm{Area}_{23} + \mathcal{O}(\varepsilon^3)$$

$$R(T) = R(0)e^{Z(T)} \tag{41}$$

If higher-order terms are considered insignificant, the following relation can be shown:

$$S(\boldsymbol{\omega}) = P^{\mathrm{SO(3)}}_{[g_1, g_2]}\mathrm{Area}_{12} + P^{\mathrm{SO(3)}}_{[g_3, g_1]}\mathrm{Area}_{31} + P^{\mathrm{SO(3)}}_{[g_2, g_3]}\mathrm{Area}_{23}$$

$$R(0)^{-1}R(T) = e^{S(\boldsymbol{\omega})}, \qquad S(\boldsymbol{V}) = \begin{bmatrix} 0 & -V_3 & V_2 \\ V_3 & 0 & -V_1 \\ -V_2 & V_1 & 0 \end{bmatrix} \tag{42}$$

As defined in Eq. (12), the projected Lie brackets are themselves vectors on which the skew-symmetric operator $S(.)$ has been performed. Thus, the net rotation of the base body of the multibody system ω is a linear combination of these vectors defined by the Lie brackets. Therefore, provided these vectors are linearly independent, for example, they satisfy the Lie algebra rank controllability condition, a unique combination of Area_{ij} exist that provide the desired reorientation. For simplicity, the inertial coordinate system can be chosen so that $R(0) = I$. For this theory to work, the constraints set forward in Eq. (1) must be satisfied. For a system such as Eqs. (32) and (33) with three controls, the parameters Area_{ij} can be expressed as

$$[\boldsymbol{Area}_{ij}] = \begin{bmatrix} \mathrm{Area}_{23} \\ \mathrm{Area}_{31} \\ \mathrm{Area}_{12} \end{bmatrix} = -\frac{1}{2}\int_0^T (\boldsymbol{u} \times \boldsymbol{\theta})\,\mathrm{d}T \tag{43}$$

The periodic control constraint appears as follows:

$$\int_0^T u_i(t)\,\mathrm{d}t = 0 \tag{44}$$

As seen in Eq. (45), these integral control constraints can be expressed as boundary constraints on a state variable. While the periodic constraint corresponds to an existing state variable, another state variable, $\boldsymbol{y}$, must be created to satisfy the area constraint. Bryson and Ho[13] give a much more detailed explanation of the use of integral constraints. Thus,

$$\dot{\boldsymbol{y}} = (\boldsymbol{u} \times \boldsymbol{\theta}) = S(\boldsymbol{u})\boldsymbol{\theta} \Rightarrow \boldsymbol{y}(0) = \boldsymbol{0}, \qquad \boldsymbol{y}(T) = -2[\boldsymbol{Area}_{ij}]$$

$$\dot{\boldsymbol{\theta}} = u \Rightarrow \boldsymbol{\theta}(0) = \boldsymbol{0}, \qquad \boldsymbol{\theta}(T) = \boldsymbol{0} \tag{45}$$

Note that, although this derivation is applied to appendage motion about $\theta_i = 0$, a simple coordinate change allows motion about any configuration $\boldsymbol{\theta}$. Additionally, one other constraint exists: that the spacecraft start from rest. For this to be true, all controls (joint angular rates) must start at zero and end at zero. For the moment, however, we will relax this constraint and reinstate it at a later time. The focus of this formulation is the minimization of the control effort required to reorient a satellite. The control effort is minimized by selecting the integral of the square of the control magnitude over the entire maneuver (from $t = 0$ to T) as the cost functional. As the control reflects the joint velocities, the cost functional is an indicator of the energy expended by the joint actuators. Thus, lowering the cost functional lowers the energy required by the spacecraft for reorientation, allowing more power to be used for primary mission objectives,

$$J = \int_0^T (u^T u)\,\mathrm{d}t \tag{46}$$

From this, the Hamiltonian equation for the system can be derived. The Lagrange multiplier μ is used to append the constraints to the cost:

$$H = \boldsymbol{u}^T\boldsymbol{u} + \boldsymbol{\mu}_y^T S(\boldsymbol{u})\boldsymbol{\theta} + \boldsymbol{\mu}_\theta^T \boldsymbol{u} \tag{47}$$

The first-order differential equations defining the Lagrange multiplier functions are defined through the derivative of the Hamiltonian with respect to the corresponding state variable. Because the artificial state variable y is not explicitly mentioned in the Hamiltonian, the multiplier μ_y is constant,

$$\frac{\mathrm{d}\boldsymbol{\mu}_y^T}{\mathrm{d}t} = -\frac{\partial H}{\partial \boldsymbol{y}} = \boldsymbol{0} \Rightarrow \boldsymbol{\mu}_y^T = \mathrm{const}$$

$$\frac{\mathrm{d}\boldsymbol{\mu}_\theta^T}{\mathrm{d}t} = -\frac{\partial H}{\partial \boldsymbol{\theta}} = -\boldsymbol{\mu}_y^T S(\boldsymbol{u}) \tag{48}$$

The optimality condition can then be used to find the control in terms of the state variables and the multiplier functions,

$$\frac{\partial H}{\partial \boldsymbol{u}} = \boldsymbol{0} = 2\boldsymbol{u}^T - \boldsymbol{\mu}_y^T S(\boldsymbol{\theta}) + \boldsymbol{\mu}_\theta^T$$

$$\therefore \boldsymbol{u} = \frac{-S(\boldsymbol{\theta})\boldsymbol{\mu}_y - \boldsymbol{\mu}_\theta}{2} = \frac{1}{2}S(\boldsymbol{\mu}_y)\boldsymbol{\theta} - \frac{1}{2}\boldsymbol{\mu}_\theta \tag{49}$$

Optimal Problem Solution

The use of Eq. (49) in the system differential equations leads to the following system:

$$\dot{\boldsymbol{y}} = -S(\boldsymbol{\theta})\boldsymbol{u} = -\frac{1}{2}S(\boldsymbol{\theta})S(\boldsymbol{\mu}_y)\boldsymbol{\theta} + \frac{1}{2}S(\boldsymbol{\theta})\boldsymbol{\mu}_\theta \Rightarrow \boldsymbol{y}(0) = \boldsymbol{0}$$

$$\boldsymbol{y}(T) = -2[\boldsymbol{Area}_{ij}], \qquad \dot{\boldsymbol{\theta}} = \frac{1}{2}S(\boldsymbol{\mu}_y)\boldsymbol{\theta} - \frac{1}{2}\boldsymbol{\mu}_\theta \Rightarrow \boldsymbol{\theta}(0) = \boldsymbol{0}$$

$$\boldsymbol{\theta}(T) = \boldsymbol{0}$$

$$\frac{\mathrm{d}\boldsymbol{\mu}_\theta}{\mathrm{d}t} = S(\boldsymbol{u})\boldsymbol{\mu}_y = -\frac{1}{2}S(\boldsymbol{\mu}_y)S(\boldsymbol{\mu}_y)\boldsymbol{\theta} + \frac{1}{2}S(\boldsymbol{\mu}_y)\boldsymbol{\mu}_\theta \tag{50}$$

On inspection, it can be seen that the $\boldsymbol{\theta}$ and $\boldsymbol{\mu}_\theta$ equations form a linear system, whereas the $\boldsymbol{y}$ equation can be solved by simple forward integration. In this case, the Laplace transform method was used to solve the linear system. Although this computation was nontrivial, after applying the boundary conditions, it yielded a compact solution for θ of the following form:

$$\boldsymbol{\theta} = \boldsymbol{A}(\boldsymbol{\mu}_y, \boldsymbol{\mu}_{\theta 0}) \sin(2\pi n/T)t + \boldsymbol{B}(\boldsymbol{\mu}_y, \boldsymbol{\mu}_{\theta 0})[\cos(2\pi n/T)(t-1)]$$

$$\boldsymbol{u} = (2\pi n/T)\boldsymbol{A}(\boldsymbol{\mu}_y, \boldsymbol{\mu}_{\theta 0}) \cos(2\pi n/T)t - (2\pi n/T)\boldsymbol{B}(\boldsymbol{\mu}_y, \boldsymbol{\mu}_{\theta 0}) \sin(2\pi n/T)t \tag{51}$$

where

$$|\boldsymbol{\mu}_y| = 2\pi n/T, \qquad \boldsymbol{A} = -(1/2|\boldsymbol{\mu}_y|)\boldsymbol{\mu}_{\theta 0}$$

$$\boldsymbol{B} = \left(1/2|\boldsymbol{\mu}_y|^2\right) S(\boldsymbol{\mu}_y)\boldsymbol{\mu}_{\theta 0} \tag{52}$$

Equation (45) imposed the terminal boundary condition on y and can be rewritten in terms of the control and state variables. The details of this and the other following calculations can be found by Cerven[12]:

$$\boldsymbol{y} = \int_0^T (\boldsymbol{u} \times \boldsymbol{\theta})\,\mathrm{d}t = -2\begin{bmatrix}\mathrm{Area}_{23}\\ \mathrm{Area}_{31}\\ \mathrm{Area}_{12}\end{bmatrix} = \frac{T^3}{16(\pi n)^2} S(\boldsymbol{\mu}_{\theta 0}) S(\boldsymbol{\mu}_{\theta 0})\boldsymbol{\mu}_y \tag{53}$$

Now five constraint equations and six unknown constants remain, meaning that any value, within bounds, of the independent constant results in an optimal solution. Through some algebraic manipulation, $|\boldsymbol{\mu}_{\theta 0}|^2$ and $\boldsymbol{\mu}_y$ can be found independent of the free constant:

$$|\boldsymbol{\mu}_{\theta 0}|^2 = \frac{16(\pi n)}{T^2}\sqrt{\mathrm{Area}_{12}^2 + \mathrm{Area}_{23}^2 + \mathrm{Area}_{31}^2} \tag{54}$$

$$\boldsymbol{\mu}_y = \frac{2\pi n}{T\sqrt{\mathrm{Area}_{12}^2 + \mathrm{Area}_{23}^2 + \mathrm{Area}_{31}^2}}\begin{bmatrix}\mathrm{Area}_{23}\\ \mathrm{Area}_{31}\\ \mathrm{Area}_{12}\end{bmatrix} = \frac{2\pi n}{T}\frac{[\boldsymbol{Area}_{ij}]}{|[\boldsymbol{Area}_{ij}]|} \tag{55}$$

When the parameter $\mu_{\theta 10}$ is chosen to be the free variable, the other constants are found to be

$$\mu_{\theta 30} = -\mu_{\theta 10}\frac{\mathrm{Area}_{23}}{\mathrm{Area}_{12}} - \mu_{\theta 20}\frac{\mathrm{Area}_{31}}{\mathrm{Area}_{12}} \tag{56}$$

$$\mu_{\theta 20} = \left(1 + \frac{\mathrm{Area}_{31}^2}{\mathrm{Area}_{12}^2}\right)^{-1}\left[-\left(\mu_{\theta 10}\frac{\mathrm{Area}_{23}}{\mathrm{Area}_{12}}\frac{\mathrm{Area}_{31}}{\mathrm{Area}_{12}}\right)\right] + \left(1 + \frac{\mathrm{Area}_{31}^2}{\mathrm{Area}_{12}^2}\right)^{-1}\left[\pm\sqrt{\left(\mu_{\theta 10}\frac{\mathrm{Area}_{23}}{\mathrm{Area}_{12}}\frac{\mathrm{Area}_{31}}{\mathrm{Area}_{12}}\right)^2 - \left(1 + \frac{\mathrm{Area}_{31}^2}{\mathrm{Area}_{12}^2}\right)\left(\mu_{\theta 10}^2\left(1 + \frac{\mathrm{Area}_{23}^2}{\mathrm{Area}_{12}^2}\right) - \frac{16(\pi n)}{T^2}|[\boldsymbol{Area}_{ij}]|\right)}\right] \tag{57}$$

By the use of this information, the controls and joint angles can be written as follows, where $\mu_{\theta 20}$ and $\mu_{\theta 30}$ are defined by Eqs. (56) and (57) and $\mu_{\theta 10}$ is independent, constrained only by $|\mu_{\theta 10}| \le |\boldsymbol{\mu}_{\theta 0}|$:

$$\boldsymbol{\theta} = -\frac{T}{2\pi n}\left\{\frac{\boldsymbol{\mu}_{\theta 0}}{2}\sin\frac{2\pi n}{T}t - \frac{[\boldsymbol{Area}_{ij}] \times \boldsymbol{\mu}_{\theta 0}}{2|[\boldsymbol{Area}_{ij}]|}\left(\cos\frac{2\pi n}{T}t - 1\right)\right\}$$

$$\boldsymbol{u} = -\frac{\boldsymbol{\mu}_{\theta 0}}{2}\cos\frac{2\pi n}{T}t + \frac{[\boldsymbol{Area}_{ij}] \times \boldsymbol{\mu}_{\theta 0}}{2|[\boldsymbol{Area}_{ij}]|}\sin\frac{2\pi n}{T}t \tag{58}$$

As already mentioned, these controls must be small (of order ε) for this theory to be applicable. As can be seen, the size of the controls depends entirely on the size of $\boldsymbol{\mu}_{\theta 0}$. As Eq. (54) shows, $|\boldsymbol{\mu}_{\theta 0}|$ is proportional to $(n^{1/2}/T)$. Therefore, when this ratio is small enough, the controls can fit the small control assumption. Practically, this means that this control is valid for any system with three controls satisfying Eqs. (32) and (33) and (41–44) provided the control frequency (defined as n/T) and reorientation time are chosen properly. As can be seen in Eq. (41), a third-order error term in the reorientation does exist, as defined in Eq. (39). This error term is of the order of $1/(n^{1/2})$ and also can be lowered through judicious choice of frequency and reorientation time.

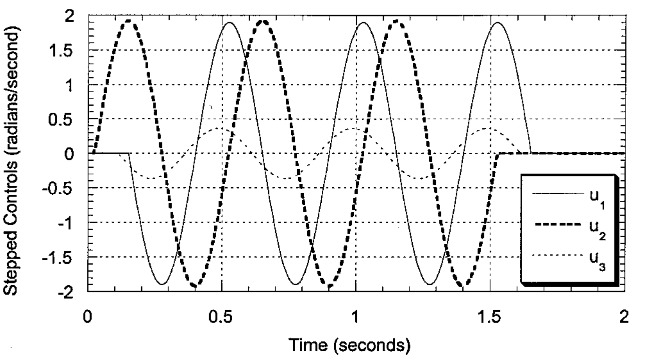

Fig. 2 Example of control stepping.

Cost Calculation

The cost for this maneuver can then easily be found. Using (46) and (51),

$$J = \int_0^T (u^T u)\,\mathrm{d}t = \left(\frac{2\pi n}{T}\right)^2 \int_0^T \left[\boldsymbol{A}\cos\frac{2\pi n}{T}t - \boldsymbol{B}\sin\frac{2\pi n}{T}t\right]^T \times \left[\boldsymbol{A}\cos\frac{2\pi n}{T}t - \boldsymbol{B}\sin\frac{2\pi n}{T}t\right]\mathrm{d}t = \frac{2(\pi n)^2}{T}(\boldsymbol{A}^T\boldsymbol{A} + \boldsymbol{B}^T\boldsymbol{B})$$

$$= \frac{T}{4}|\boldsymbol{\mu}_{\theta 0}|^2 = \frac{4\pi n}{T}\sqrt{\mathrm{Area}_{12}^2 + \mathrm{Area}_{23}^2 + \mathrm{Area}_{31}^2} \tag{59}$$

As can be expected, the final cost varies directly with the magnitude of the reorientation as shown by the area terms, as well as the frequency of the controls. However, these calculations did not take into account the assumption of the spacecraft starting at rest, or that $\boldsymbol{u} = \boldsymbol{0}$ at the beginning and end of the maneuver. This can be accomplished by stepping in the controls and stepping them out one at a time, as can be seen in Fig. 2.

By keeping the time each control operates the same, the cost remains unchanged. However, there does exist a penalty in the accuracy of the resulting reorientation due to the loss of time that all three controls were coupled together. This time of not operating simultaneously is no more than $T/(2n)$. From this, the difference in final orientation is found to be of order $1/(2n)$. This is negligible in comparison to the error of order $1/(n^{1/2})$ due to the higher-order terms when n is large. To satisfy the small control assumption, this must be the case. Thus, the cost in pointing accuracy is negligible, and the stepped controls are also considered an optimal solution to the averaged system.

An appreciation for the usefulness of this optimization can be obtained through a comparison of cost to other controls utilizing the same averaging theory. For a space robot with three actuated joints, Rui[6] proposed the control

$$\boldsymbol{u} = \frac{2\sqrt{n}}{T} \times \begin{bmatrix} -\frac{\text{Area}_{31}}{a_{31}}\sin\left(\frac{2\pi nt}{T}\right) + \frac{\text{Area}_{12}}{a_{22}}\sin\left(\frac{4\pi nt}{T}\right) \\ \frac{\text{Area}_{23}}{a_{31}}\sin\left(\frac{2\pi nt}{T}\right) + a_{22}\pi\cos\left(\frac{4\pi nt}{T}\right) - a_{22}\pi\cos\left(\frac{6\pi nt}{T}\right) \\ a_{31}\pi\cos\left(\frac{2\pi nt}{T}\right) - a_{31}\pi\cos\left(\frac{6\pi nt}{T}\right) \end{bmatrix} \tag{60}$$

When the definition of cost defined in Eq. (46) is used, J_{rui} is found to be a function of the squares of two free variables a_{22} and a_{31}:

$$J_{\text{rui}} = \frac{2n}{T}\left[\frac{\text{Area}_{31}^2 + \text{Area}_{23}^2}{a_{31}^2} + \frac{\text{Area}_{12}^2}{a_{22}^2} + 2\pi^2\left(a_{22}^2 + a_{31}^2\right)\right] \geq 0 \tag{61}$$

The relative cost, or the difference between this and the optimal cost found in Eq. (59), can be expressed as

$$J_{\text{rui}} - J = \frac{2n}{T}\left[\frac{\text{Area}_{31}^2 + \text{Area}_{23}^2}{a_{31}^2} + \frac{\text{Area}_{12}^2}{a_{22}^2} + 2\pi^2\left(a_{22}^2 + a_{31}^2\right)\right] - \frac{4\pi n}{T}\sqrt{\text{Area}_{12}^2 + \text{Area}_{23}^2 + \text{Area}_{31}^2} \tag{62}$$

Rui's[6] cost given in Eq. (61) has four minimums: one in each quadrant with the values for a_{22} and a_{31} given as

$$[a_{22}, a_{31}] = \left[\pm\frac{\sqrt{2}}{2}\sqrt{\frac{\sqrt{2}\sqrt{\text{Area}_{12}^2}}{\pi}}, \pm\frac{\sqrt{2}}{2}\frac{\sqrt{2}\sqrt{\text{Area}_{23}^2 + \text{Area}_{31}^2}}{\pi}\right] \tag{63}$$

Therefore, the smallest difference between costs can be shown to be

$$(J_{\text{rui}} - J)_{\min} = \frac{4\pi n}{T}\left\{\sqrt{2}\sqrt{\text{Area}_{23}^2 + \text{Area}_{31}^2} + \sqrt{2}\sqrt{\text{Area}_{12}^2} - \sqrt{\text{Area}_{12}^2 + \text{Area}_{23}^2 + \text{Area}_{31}^2}\right. \tag{64}$$

When the triangle inequality is used, it can be seen that

$$\sqrt{\text{Area}_{23}^2 + \text{Area}_{31}^2} + \sqrt{\text{Area}_{12}^2} \geq \sqrt{\text{Area}_{12}^2 + \text{Area}_{23}^2 + \text{Area}_{31}^2} \tag{65}$$

Therefore,

$$(J_{\text{rui}} - J)_{\min} \geq 0 \tag{66}$$

and the solution represented in Eq. (58) is shown to provide a more efficient reorienting algorithm.

Example

A four-link revolute-joint spacecraft comparable to that given by Rui[6] and geometrically similar to that given by Coverstone-Carroll and Wilkey[5] was selected to test the control algorithm. It consists of three axially symmetric links attached to one another and an axially symmetric base body through revolute joints parallel to the x axis of each link. The specific geometric and mass properties of these links are presented in Eqs. (67) and (68). The beginning orientation of each of the bodies is given by 3–2–1 Euler angles [relative to $(i-1)$th body frame], where θ is the revolute joint angle. The initial and desired final base body orientations (relative to the inertial frame) are given by (69) and (70). Thus,

$$I_0 = \begin{bmatrix} 1.2 & 0 & 0 \\ 0 & 6.6 & 0 \\ 0 & 0 & 6.6 \end{bmatrix}, \qquad m_0 = 58.2, \qquad \begin{matrix} l_0 = 0.8 \\ r_0 = 0.2 \end{matrix}$$

$$I_1 = \begin{bmatrix} 4.0 & 0 & 0 \\ 0 & 4.0 & 0 \\ 0 & 0 & 0.6 \end{bmatrix}, \qquad m_1 = 37.5, \qquad \begin{matrix} l_1 = 0.6 \\ r_1 = 0.05 \end{matrix}$$

$$I_2 = \begin{bmatrix} 3.5 & 0 & 0 \\ 0 & 3.5 & 0 \\ 0 & 0 & 0.3 \end{bmatrix}, \qquad m_2 = 28.4, \qquad \begin{matrix} l_2 = 0.6 \\ r_2 = 0.05 \end{matrix}$$

$$I_3 = \begin{bmatrix} 3.8 & 0 & 0 \\ 0 & 3.8 & 0 \\ 0 & 0 & 0.35 \end{bmatrix}, \qquad m_3 = 30.0, \qquad \begin{matrix} l_3 = 0.6 \\ r_3 = 0.05 \end{matrix} \tag{67}$$

Here all values are in degrees,

$$\psi_1 = 90, \quad \psi_2 = 90, \quad \psi_3 = 45, \quad \phi_1 = 0, \quad \phi_2 = 0$$

$$\phi_3 = 0, \quad \theta_1 = -30, \quad \theta_2 = 60, \quad \theta_3 = 60 \tag{68}$$

$$\psi_0 = 0, \quad \phi_0 = 0, \quad \theta_0 = 0 \tag{69}$$

$$\psi_f = 0, \quad \phi_f = -60, \quad \theta_f = 0 \tag{70}$$

When a $T = 200$-s reorientation time and $n = 400$ cycles are chosen, with an arbitrarily chosen $\mu_{\theta 10} = -3.611$ free variable, the controls become

$$u_1 = 1.8057\cos(12.566t) + 0.5964\sin(12.566t)$$

$$t_{\text{start}} = 0.15038$$

$$u_2 = -0.5749\cos(12.566t) + 1.8333\sin(12.566t)$$

$$t_{\text{start}} = 0.02418$$

$$u_3 = 0.3602\cos(12.566t) - 0.0634\sin(12.566t)$$

$$t_{\text{start}} = 0.11113 \tag{71}$$

with u values in radian per second and t_{start} values in seconds.

Each of these controls was phased in at t_{start} and phased out at $200\text{ s} + t_{\text{start}}$. Because the system is driftless, this guarantees the joint and base body rates are zero at the beginning and end of the maneuver. The base body rates (30) were calculated from the controls using a C preprocessor. The system state history was computed from Eq. (10) through a Fehlberg fourth–fifth-order Runge–Kutta algorithm in Maple version 5.4 with the absolute error set to 10^{-8}. The resulting final orientation (deg) of the actual system was found to be

$$\psi_f = -5.06, \quad \phi_f = -60.21, \quad \theta_f = -6.22 \tag{72}$$

Figure 3 shows the initial and final spacecraft orientations, whereas Fig. 4 shows the orientation history of the base body and its net secular variation. The error between this result and the desired orientation is of the order $1/(n^{1/2})$ and, thus, fits theoretical expectations. The cost of this reorientation was 744 m^2/s, which is a great

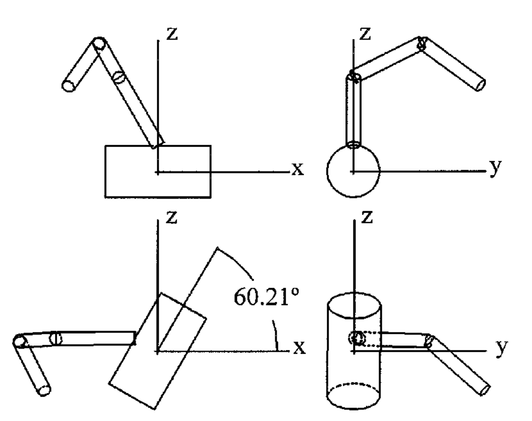

Fig. 3 Initial and final orientations of the spacecraft.

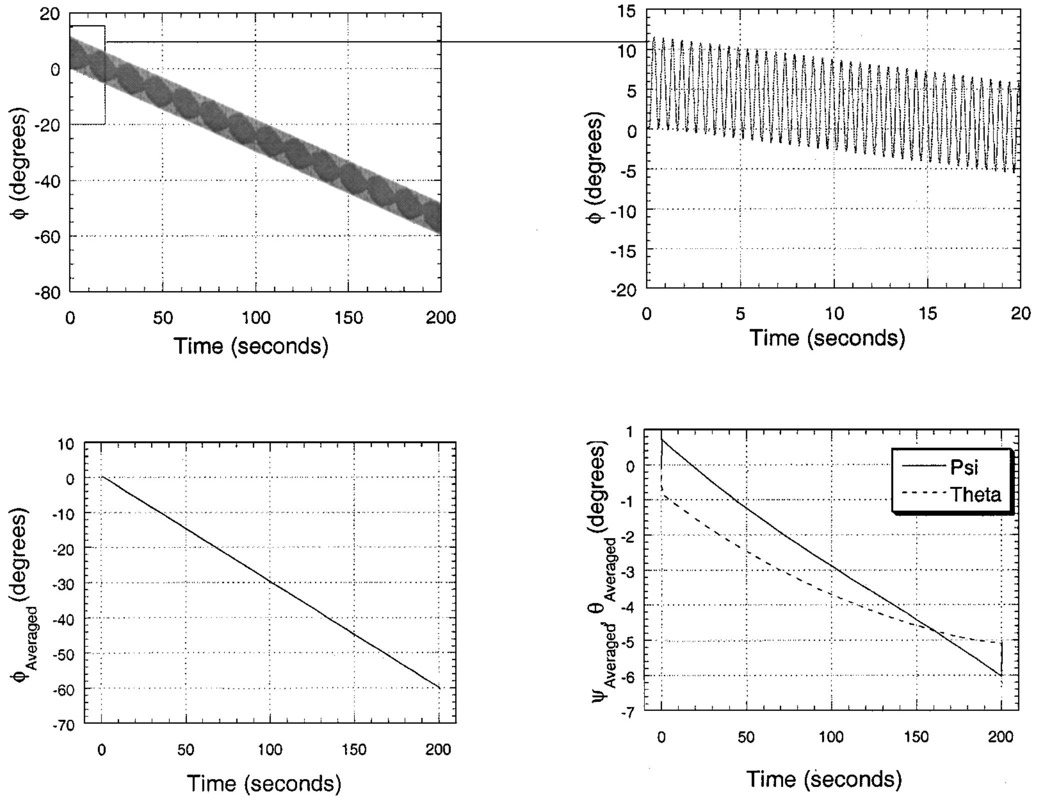

Fig. 4 Simulation base body 3–2–1 (ψ, ϕ, θ) Euler angles.

improvement in comparison to the Rui[6] control cost of 2397 m^2/s for the same reorientation.

Conclusions

A more efficient application of small periodic controls to secular variations in four-link multibody systems is developed. These secular variations are shown to exist and be usable in driftless systems ranging from the general vector differential equation to systems on Lie groups and multibody systems. For the case in which three revolute joint controls are used in a four-body system, a relatively simple and elegant optimization is derived using properties of the rotation matrix. This yields an analytic optimal control that minimizes the control effort required for reorientation. The optimal control law is compared to previously developed control algorithms for the four-link spacecraft to illustrate the advantages.

Acknowledgments

This material is based on work supported under a National Science Foundation Graduate Fellowship. Thanks also are due to Professor Francesco Bullo and Scott Zimmer for their support in this research.

References

[1]Kane, T. R., and Scher, M. P., "A Dynamical Explanation of the Falling Cat Phenomenon," *International Journal of Solids and Structures*, Vol. 5, No. 7, 1969, pp. 663–670.

[2]Kane, T. R., and Scher, M. P., "Human Self-Rotation by Means of Limb Movements,"*Journal of Biomechanics*, Vol. 3, No. 1, 1970, pp. 39–49.

[3]Krishnaprasad, P. S., "Geometric Phases and Optimal Reconfiguration for Multibody Systems," *Proceedings of American Control Conference*, Inst. of Electrical and Electronics Engineers, New York, 1990, pp. 2440–2444.

[4]Fernandes, C., Gurvits, L., and Li, Z., "Near-Optimal Nonholonomic Motion Planning for a System of Coupled Rigid Bodies," *IEEE Transactions on Automatic Control*, Vol. 39, No. 3, 1994, pp. 450–463.

[5]Coverstone-Carroll, V. L., and Wilkey, N. M., "Optimal Control of a Satellite-Robot System Using Direct Collocation with Nonlinear Programming," *Acta Astronautica*, Vol. 36, No. 3, 1995, pp. 149–162.

[6]Rui, C., "Dynamics and Nonlinear Attitude Control of Multibody Space Systems," Ph.D. Thesis, Dept. of Aerospace Engineering, Univ. of Michigan, Ann Arbor, MI, 1997.

[7]Leonard, N. E., and Krishnaprasad, P. S., "Motion Control of Drift-Free, Left-Invariant Systems on Lie Groups," *IEEE Transactions on Automatic Control*, Vol. 40, No. 9, 1995, pp. 1539–1554.

[8]Leonard, N. E., and Krishnaprasad, P. S., "Averaging for Attitude Control and Motion Planning," *Proceedings of the 32nd IEEE Conference Decision and Control*, Inst. of Electrical and Electronics Engineers, New York, 1993, pp. 3098–3104.

[9]Leonard, N. E., "Averaging and Motion Control of Systems on Lie Groups," Ph.D. Dissertation, Dept. of Electrical Engineering, Univ. of Maryland, College Park, MD, 1994.

[10]Brockett, R. W., "On the Rectification of Vibratory Motion," *Sensors and Actuators*, Vol. 20, No. 1–2, 1989, pp. 91–96.

[11]Rui, C., Kolmanovsky, I., and McClamroch, N. H., "Three Dimensional Attitude and Shape Control of Spacecraft with Appendages and Reaction Wheels," *Proceedings of the 32nd IEEE Conference on Decision and Control*, Inst. of Electrical and Electronics Engineers, New York, 1998, pp. 4176–4181.

[12]Cerven, W. T., "Optimal Control of a Multibody Spacecraft Using Averaging Theory," M.S. Thesis, Dept. of Aeronautical and Astronautical Engineering, Univ. of Illinois, Urbana–Champaign, IL, May 1999.

[13]Bryson, A. E., and Ho, Y., *Applied Optimal Control: Optimization, Estimation, and Control*, Hemisphere, New York, 1975, pp. 47–98.